Chain Dynamics in the Crystalline α-Phase of Poly(vinylidene fluoride) by Two-Dimensional Exchange ^{2}H NMR

Jérôme Hirschinger,† Dieter Schaefer, and Hans Wolfgang Spiess*

Max-Planck-Institut für Polymerforschung, Postfach 3148, D-6500 Mainz, Germany

Andrew J. Lovinger

AT&T Bell Laboratories, Murray Hill, New Jersey 07974

Received September 6, 1990; Revised Manuscript Received November 20, 1990

ABSTRACT: Two-dimensional (2D) exchange deuteron NMR has been applied to study the ultraslow chain motion in the crystalline α-phase of poly(vinylidene fluoride) and specifically its very unusual α-relaxation that occurs in the crystalline regions at ca. 370 K. Without the need for interfacing a model of motion, this technique demonstrates that the chain motion associated with this α-relaxation is reorienting the C–^{2}H bond directions by uniquely defined angles of 67 or 113°. Owing to the high angular resolution of 2D exchange ^{2}H NMR (±0.5°), it is shown that these reorientation angles are most consistent with the crystalline structure of Takahashi et al. (*Macromolecules* **1983**, *16*, 1588). Considering also the dielectric relaxation results of Miyamoto et al. (*J. Polym. Sci.: Polym. Phys. Ed.* **1980**, *18*, 597), we arrive at a *unique* conclusion about the dynamics: the chain motion is characterized by an electric dipole moment transition only along the molecular direction and by a conformational change TGTḠ ↔ ḠTGT, yielding a reorientation angle of 113° for the C–^{2}H bond directions.

Introduction

Poly(vinylidene fluoride) (PVF_2) has attracted much scientific and technological interest because it combines remarkable piezoelectric and pyroelectric properties with the excellent processability and mechanical strength of a crystalline thermoplastic.[1] It has rapidly become clear that the origins of these extraordinary electrical properties are almost exclusively due to reorientation mechanisms of the electric dipole moments formed by the C–F bonds.[1,2] Hence, it is of primary importance to examine at the *segmental length scale* how the conformation of PVF_2 chains responds to applied electrical, mechanical, or thermal treatments. The ability of PVF_2 to undergo conformational changes is reflected in the abundance of polymorphic phases. Indeed, from the most common α-phase, the β-, γ, and δ-phases can be prepared under action of mechanical stress, heat, or electrical field, respectively. A major question concerning PVF_2 is the mechanism of its mechanical and dielectric relaxations. Specifically, in the PVF_2 α-phase, it has been shown by several techniques[3-7] that the high-temperature (or "α") relaxation is caused by molecular motion in the crystalline domains. Notably, McBrierty et al.[6] could interpret their ^{1}H and ^{19}F NMR relaxation data by two models: rotation of crystalline chains in the vicinity of defects and rotational oscillation of restricted amplitude of all chains about the chain axis. On the other hand, from dielectric relaxation, Miyamoto et al.[5] proposed a mechanism in which the reversal of only the dipole-moment component *along* the chain axis takes place. This has received support from X-ray analysis.[7] However, the energy for a solitary-wave reversal of the dipole moment along the molecular direction was calculated[8] to be much higher than found in ref 5.

In order to distinguish among these competing interpretations, we have applied pulsed ^{2}H NMR, which probes the orientation of individual C–^{2}H bonds and which has proved to be a powerful tool for studying molecular order and dynamics.[9] Furthermore, the recently developed two-dimensional (2D) ^{2}H and ^{13}C NMR techniques[10-17] have been shown to provide much more *direct* information than is available from conventional one-dimensional (1D) experiments.[9] Also, note that ^{2}H NMR is particularly well suited to the study of PVF_2 since the presence of both ^{1}H and ^{19}F nuclei renders the application of solid-state high-resolution NMR[18] difficult. Doverspike et al.[19] have already used 1D ^{2}H NMR in PVF_2 to measure the effect of poling on the molecular order in the ferroelectric β-phase.

In the present paper, we use 2D exchange ^{2}H NMR in order to characterize the ultraslow molecular motion in the crystalline α-phase of PVF_2. The motional mechanism is then deduced by comparison with available crystallographic[7,20-23] and dielectric relaxation[3-5] data.

Two-Dimensional Exchange NMR

In this section, we give a brief qualitative description of the 2D exchange ^{2}H NMR experiment and the information available from it. The theory and applications of 2D exchange ^{2}H and ^{13}C NMR in both static and rotating samples are presented in detail in the original literature.[11-16] A simplified description of the experiment and its application to study chain mobility in crystalline and amorphous polymers is also given in ref 17.

Anisotropic Interaction. The ^{2}H NMR spectrum is dominated by the coupling of the electric field gradient with the nuclear electric quadrupole moment. If the electric field gradient tensor (FGT) is axially symmetric, as is a good approximation in ^{2}H NMR, the orientation dependence of the NMR frequency in the rotating frame is given by[24]

$$\omega = \pm\delta(3\cos^2\theta - 1)/2 = \pm\delta P_2(\cos\theta) \qquad (1)$$

where θ is the angle between the unique principal axis of the FGT, i.e., the C–^{2}H bond direction, and the static magnetic field $\mathbf{B}_0$. The constant $\delta = 3e^2qQ/4\hbar$ specifies the strength of the anisotropic quadrupolar interaction ($\delta/2\pi \simeq 125$ kHz for aliphatic polymer chains). For isotropic powders, an inhomogeneously broadened line shape (Pake diagram) results with characteristic singularities at $\omega = \pm\delta/2$ for $\theta = 90°$.

† Present address: Institut de Chimie, BP 298-R8, 67008 Strasbourg Cedex, France.

0024-9297/91/2224-2428$02.50/0

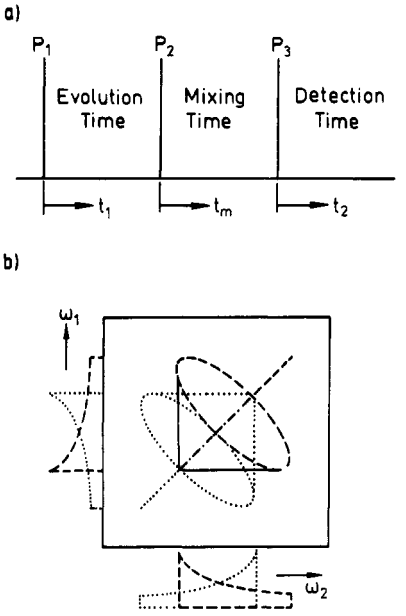

Figure 1. (a) Basic three-pulse sequence used in 2D exchange NMR. In practice, an additional fourth pulse is included to overcome the receiver deadtime.[11] (b) Schematic 2D exchange ^2H spectrum of a powder for a definite reorientation angle Θ = 109.4°: elliptical ridge (- - -) and 90° ridge (—) for one ^2H NMR transition. The second transition (···) gives the mirror symmetry about the antidiagonal.

Three-Pulse Sequence. Two-dimensional exchange NMR is a particular application of 2D spectroscopy[25] especially designed to study slow dynamic processes with rates that are too low to affect the 1D line shapes. For deuterons (I = 1), a three-pulse sequence is used[11-14] (Figure 1a): after the application of a first pulse P_1, during the evolution time t_1, the ^2H magnetization for a given molecular orientation in the rotating frame evolves with a frequency ω_e (cf. eq 1), which is then stored by a second pulse P_2 at time $t = t_1$. During the mixing time t_m, a molecular reorientation due to slow motion is generally reflected by a change in the NMR frequency according to eq 1. This new frequency ω_d is probed in the subsequent detection time t_2 by the application of a third pulse P_3 bringing back ^2H magnetization in the transverse plane. By incrementing t_1, a 2D data set is obtained. After 2D Fourier transformation relative to t_1 and t_2, cross-peaks of equal intensity appear at $(\omega_1, \omega_2) = (\omega_e, \omega_d)$ and (ω_d, ω_e), thus yielding a spectrum symmetrical to the 2D plane diagonal $\omega_1 = \omega_2$. Because of the presence of two ^2H NMR transitions, there is also a mirror symmetry about the antidiagonal $\omega_1 = -\omega_2$. Hence, four cross-peaks are generally observed in a single-crystal experiment. The 2D spectrum is then a direct visual representation of the pathways of the mixing process, i.e., the molecular motion. By systematic variation of t_m, the dynamic process can be followed in *real time*.

Information Available from Powders. In the case of an isotropic powder sample, after a single reorientation angle Θ during t_m, the C–^2H bonds having the same initial orientation at an angle θ_e from $\mathbf{B}_0$ will lie on a cone whose symmetry axis is along the initial orientation. Thus, the ω_2-slice of the 2D exchange pattern going through $\omega_1 = \omega_e = \pm\delta P_2(\cos\theta_e)$ will be a line shape given by a conical distribution of orientations. Such a line shape can be calculated analytically[8] and has singularities at $\omega_2 = \pm\delta P_2(\cos(\theta_e + \Theta))$, at $\omega_2' = \pm\delta P_2(\cos(\theta_e - \Theta))$, and, if $\theta_e + \Theta \geq \pi/2$, also at $\omega_2'' = \pm\delta/2$. Of course, the C–^2H bonds that have the same orientation during t_1 and t_2 (Θ = 0) will not result in any off-diagonal exchange signal but will give rise to a Pake diagram along the diagonal of the 2D spectrum. On the other hand, for $\Theta \neq 0$, the singularities ω_2, ω_2', and ω_2'' form characteristic off-diagonal exchange ridge patterns (Figure 1b). The first two singularities ω_2 and ω_2' are of particular interest since they form ellipses from which the reorientational angle Θ can be directly extracted.[11-17] The singularities at ω_2'' form straight lines parallel to the ω_1-frequency axis, which extend from the diagonal until they reach the corresponding ellipse (Figure 1b). Similar ridges are obtained along the ω_2-axis at $\omega_1'' = \pm\delta/2$. It is then remarked that all these straight ridges with ω_1 or $\omega_2 = \pm\delta/2$ are associated with C–^2H bond orientations lying at 90° from $\mathbf{B}_0$ before or after the jump so that the positions of these "90° ridges" are independent of the reorientation angle Θ. This fact explains why the 90° ridges are still observable if the motional process involves a broad reorientational angle distribution (RAD) $P(\Theta)$ (e.g., isotropic diffusion) while the ellipses are smeared out in this case.[13,14] By analysis of the 2D spectrum, $P(\Theta)$ and, thus, the geometry of the motion can *directly* be measured, i.e., without any model consideration.[16] However, due to the form of the NMR frequency orientation dependence (eq 1), one cannot distinguish between the jump angle Θ and its complement 180° – Θ. Thus, $P(\Theta)$ is contracted to the interval [0–90°].[12-16]

Experimental Section

Perdeuterated PVF_2 has been prepared by polymerization of separately synthesized and isolated $CF_2{=}CD_2$ as described in ref 26. Its viscosity-average molecular weight is 390 000. In principle, the statistical packing in the deuterated polymer may differ from that of the standard, non-deuterated material. In order to check the crystal modification, X-ray diffractograms of the deuterated sample were taken, exhibiting a structure typical of the α-phase, but with higher crystallinity. Therefore, our NMR results (although in the strictest sense valid only for the deuterated material) are discussed below in terms of the various models proposed for protonated PVF_2. DSC indicates a substantially higher melting point and enthalpy of fusion than the commercial (protonated) counterparts. This is believed to be a result of the increased crystallinity of deuterated samples, which in turn stems from the reduced content of branching and regioirregular defects in deuterated chains.[26,27]

The NMR experiments were performed on a Bruker CXP 300 spectrometer operating at a ^2H resonance frequency of 46.07 MHz. The duration of a 90° pulse was 2.1 μs. By applying the pulse sequences described in detail in ref 11, two time-domain data matrices of 40 × 128 complex values were obtained. These sequences, in addition to different phase cycles of the three-pulse sequence of Figure 1a with P_1 = 90°, $P_2 = P_3$ = 54.7° contain a refocusing 90° pulse in the detection period. The finite pulse widths lead to distortions in the 2D NMR spectra. Therefore, the simulation presented below includes these distortions through multiplication of the frequency data in both dimensions by correction factors $\sin x/x$ for each pulse, where x is proportional to the pulse length.[25] The effective pulse length used for this correction is shorter than the experimental one by 15%. The spectral width was 312.5 kHz in both dimensions, and the repetition time was 3 s. The measuring time of a 2D spectrum then ranged from 11 to 72 h (see Figures 2 and 3). The 2D data sets were subsequently processed according to ref 11 to obtain pure phase 2D spectra. The dimension of the data sets was increased to 128 × 128 by zero filling prior to Fourier transformation after proper Gaussian apodization. The temperature was controlled by a Bruker VT 1000 temperature unit.

Results and Discussion

Geometry of the Motion. Figure 2a,b shows the 2D exchange ^2H NMR spectrum of α-PVF_2 at 370 K for t_m = 200 ms. At this temperature, the spin–lattice relaxation (T_1) decay is well fitted by a two-exponential curve with

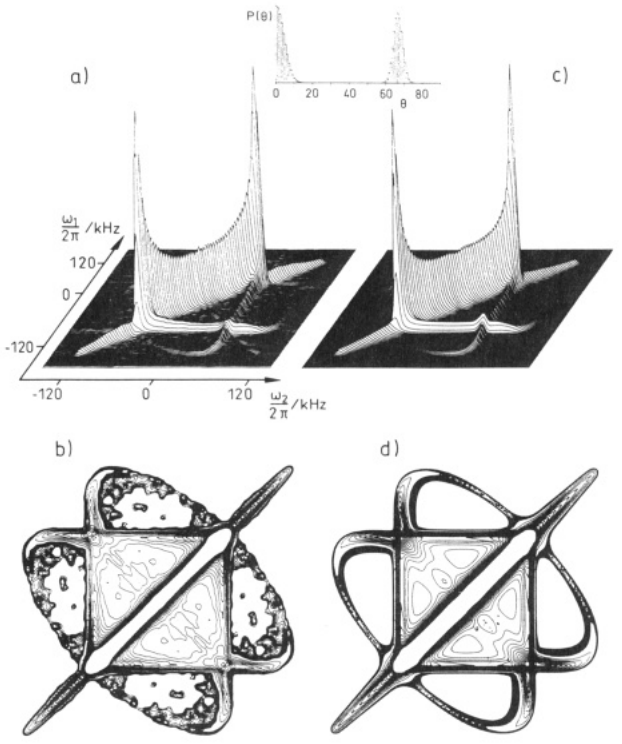

Figure 2. 2D exchange ^2H NMR spectrum of α-PVF_2. (a) Experiment at 370 K with a mixing time t_m = 200 ms (measuring time: 72 h). (b) Contour plot of a. (c) Simulation considering a Gaussian jump angle distribution of ±5° width around Θ = 0° and ±3° around Θ = 67°. The insert shows the corresponding reorientation angle distribution (RAD) $P(\Theta)$. (d) Contour plot of c.

time constants 20 ms and 2 s. The fast relaxing component representing about 40% of the magnetization is associated with the motionally averaged line shape arising from the amorphous material (see Figure 3). Thus, at t_m = 200 ms, this part of the magnetization has decayed and only the slowly relaxing crystalline signal is detected. The relatively short repetition time (3 s) was chosen as a compromise to reduce the measuring time and nevertheless observe about 80% of the crystalline magnetization. Clearly, the ultraslow motion discussed below cannot account for a T_1 value of about 2 s since one would expect T_1 to be of the order of minutes as in molecular crystals.[28] Hence, as already observed in other crystalline polymers,[29,30] there must be small angle fluctuations with a rate quite close to the Larmor frequency. Note that, without the presence of such a fast motion, 2D ^2H NMR would be impossible due to a prohibitively long measuring time.

The 2D spectrum displays a well-defined Pake diagram along the diagonal. More interestingly, one observes elliptical exchange ridges in addition to the 90° ridges (Figure 2a,b). The 90° ridges are found within experimental accuracy parallel to the ω_1- and ω_2-axes, thus demonstrating that the FGT tensor is effectively axially symmetric ($\eta \leq 0.01$).[11] The RAD $P(\Theta)$ deduced from the comparison with the calculated spectra (Figure 2c,d) is also plotted. The RAD exhibits two peaks centered at Θ = 0 and 67° (Figure 2c). The latter indicates a jump motion of the C–^2H bond by an angle of 67 or 180 − 67 = 113° in the crystal lattice. $P(\Theta)$ also indicates an uncertainty of the reorientational angle of ±3°. Since the angular resolution in 2D exchange ^2H NMR is as high as ±0.5°,[16] the broader RAD in PVF_2 clearly reflects the nonideal packing in a polymer crystal as already observed in isotactic polypropylene.[17] As demonstrated in the next section, the spectrum of Figure 2 corresponds to the "final state" RAD[12-14] reached for $t_m \gg \tau_c$, the correlation time of the motion. Since the diagonal and off-diagonal parts of the spectrum have about equal intensities, it is concluded that the jump motion involves only two sites.[12-14,28]

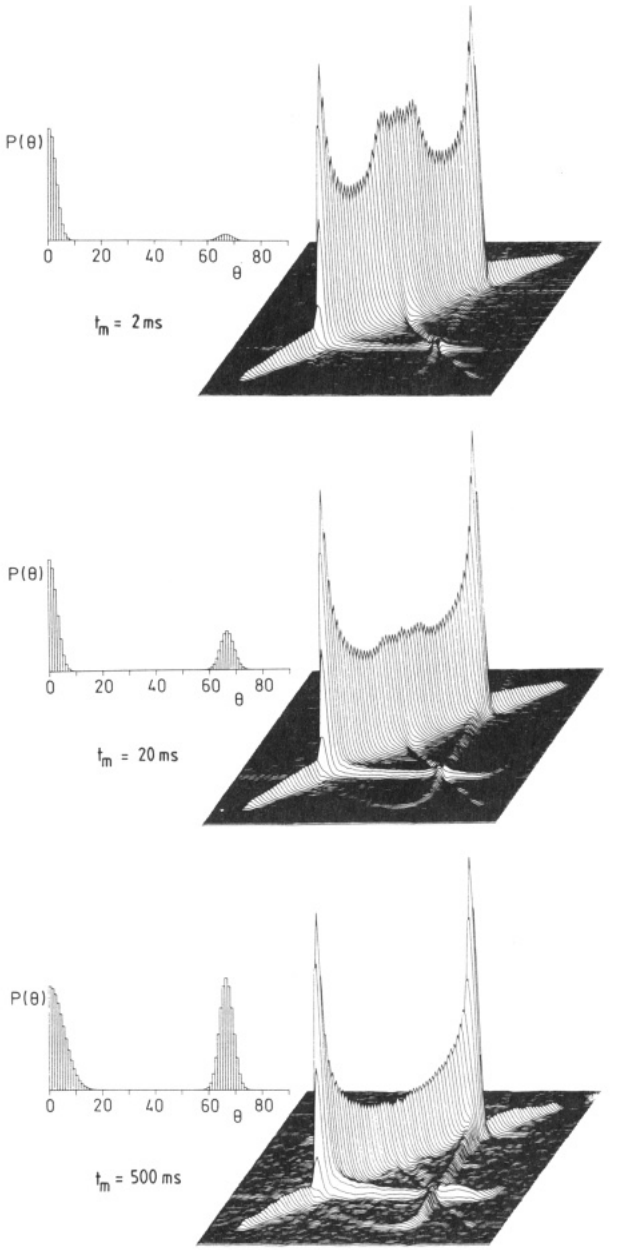

Figure 3. 2D exchange ^2H NMR spectra of α-PVF_2 at T = 370 K with varying mixing time t_m = 2, 20, and 500 ms. The measuring time is 11, 26, and 43 h, respectively. In the inserts are fitted the corresponding RAD of the crystalline motion.

Time Scale of the Motion. The emphasis of the current investigation concerns the geometry of the motion. From 2D NMR spectra, however, the time scale of the motion can also be evaluated by varying the mixing time t_m.[12-14,28] Figure 3 shows the 2D spectra at 370 K for t_m = 2, 20, and 500 ms. For the two smaller mixing times, one clearly observes the contribution of the fast relaxing amorphous line shape in the center of the diagonal. As t_m increases, the intensity of the off-diagonal signals increases relative to the diagonal, reflecting the time scale of the motion. For each spectrum, disregarding the diagonal motionally averaged amorphous signal, it is then possible to extract the RAD corresponding to the crystalline motion. Obviously, there is no significant increase in exchange intensity when increasing t_m from 200 to 500

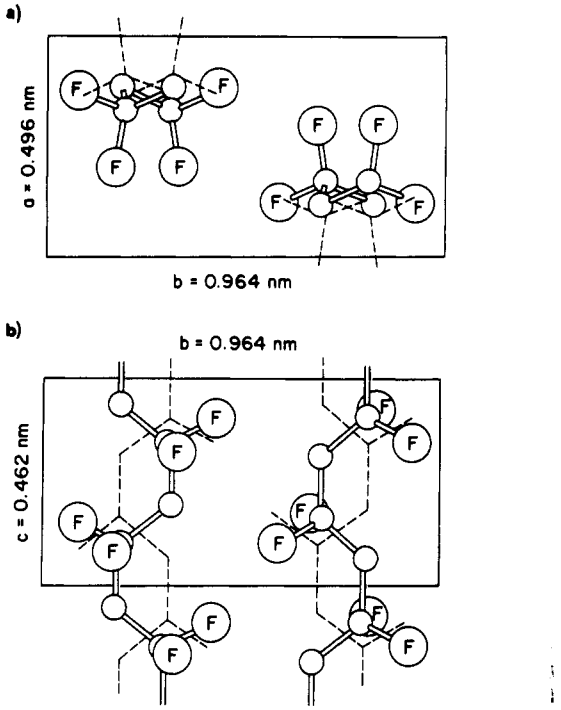

Figure 4. Unit cell of α-PVF_2 according to the structure of ref 23. (a) c-axis projection. (b) a-axis projection. The hydrogen atoms have been omitted for clarity.

ms, demonstrating that the final state RAD is reached, at least, for $t_m \geq 200$ ms. From the RAD at $t_m = 2$ and 20 ms, we calculate that the correlation time of the two-site jump motion τ_c is 20 ± 5 ms at 370 K. Previous dielectric relaxation studies[3,4] report shorter correlation time values (0.1–1 ms) for the α-relaxation at 370 K. However, it has been observed that the position of the loss maximum for the α-relaxation is strongly shifted toward higher temperature (i.e., longer correlation times) with decreasing level of chemical defects (head–head or tail–tail junctions).[3] Since deuterated samples of PVF_2 have been shown to have a much lower content of reversed monomer units (≈2.8%) than the protonated samples (≈3.5–6%),[26] we conclude that the two-site jump motion observed by 2D NMR is, indeed, responsible for the α-relaxation process.

Models of Molecular Motion. As described above, 2D exchange ^2H NMR demonstrates *without any model assumptions* that the C–^2H bonds in the crystalline α-phase of PVF_2 are slowly jumping between two orientations separated by a mean angle of 67 or 113°. In this section, therefore, we examine all the possible chain reorientations that are compatible with these jump angles and the crystalline structure.

There have been several X-ray studies of PVF_2 in its α-phase.[20–23] The chain conformation is well established as essentially TGTḠ[20,23] or a distorted analogue.[21,22] The unit cell is (at least metrically) orthorhombic with a = 0.496 nm, b = 0.964 nm, and c (molecular axis) = 0.462 nm, and the chains are overall packed in an antipolar and antiparallel manner (see Figure 4). However, the precise packing of the chains is quite complex since it was recently shown to involve a disorder. Bachmann and Lando[22] were the first to report a statistical up–down disorder, with each chain having a 50% probability of "up" or "down" orientation along the c axis. Subsequently, Takahashi et al.[23] proposed a more elaborate disorder between four possible chain orientations in the unit cell. In the α-phase, two components of the electric dipole moment must be taken into consideration: a component $\mu_\perp$ (perpendicular

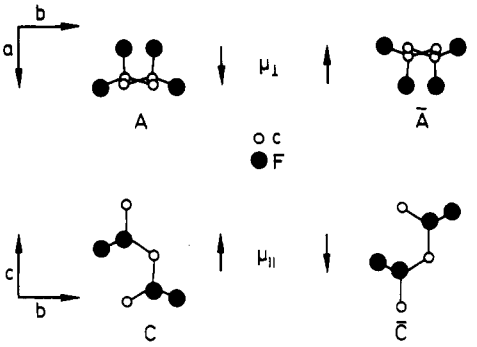

Figure 5. Four polarization states of α-PVF_2, according to ref 23. The symbols A and Ā denote the dipole-moment orientation in the ab plane ($\mu_\perp$), and the symbols C and C̄ denote the up and down orientation ($\mu_\parallel$), respectively. Hydrogen atoms have been omitted for clarity.

Table I

motion	conform change	transition type	reorientation angle θ for C–^2H bonds (jump angle), deg ref 20	refs 21, 22	ref 23
1	TGTḠ ↔ TGTḠ	AC ↔ AC	0	0	0
2	TGTḠ ↔ TGTḠ	AC ↔ ĀC	129; 180	148; 171	128; 178
3	TGTḠ ↔ TḠTG	AC ↔ AC	109	132	112
4	TGTḠ ↔ TḠTG	AC ↔ ĀC	71	45	67
5	TGTḠ ↔ GTḠT	AC ↔ AC̄	51; 0	32; 9	52; 2
6	TGTḠ ↔ GTḠT	AC ↔ $\overline{AC}$	180	180	180
7	TGTḠ ↔ ḠTGT	AC ↔ AC̄	109	135	113
8	TGTḠ ↔ ḠTGT	AC ↔ $\overline{AC}$	71	48	68

to the molecular axis) in the direction of the a axis, and the other one $\mu_\parallel$ (parallel to the molecular axis) in the direction of the c axis. The orientation of $\mu_\perp$ can then be "right" (A) or "left" (Ā) while $\mu_\parallel$ can be "up" (C) or "down" (C̄) (Figure 5), using the terminology introduced by Takahashi et al.[23] They reported existence probabilities at room temperature as 54% for the AC orientation, 29% for AC̄, 10% for ĀC, and 7% for $\overline{AC}$. A dipole-moment change in the α-phase of PVF_2 can then be described by transitions between the four chain polarization states AC, AC̄, ĀC, and $\overline{AC}$. Clearly, transitions between these states require molecular reorientations. It is easily demonstrated that there are 16 different reorientations for a pair of C–^2H bonds between the 4 polarization states. However, 8 of these 16 motions involve a 180° rotation about the a or b crystal axis, implying chain break or chain reentry, and, therefore, must be ruled out. We are then left with the eight physically possible motions that are listed in Table I. Furthermore, it is seen that there are only four possible conformational changes (second column of Table I), each of which leads to two polarization transitions (third column of Table I) whose final states are related by a 180° rotation about the c axis. Note that motion 1 characterized by equal initial and final states (no apparent motion) is given here for completeness. In the fourth to the sixth columns of Table I, we have calculated the jump angles Θ associated with each molecular motion 1–8 according to the atomic coordinates derived in the relevant X-ray studies. These were done, in chronological order, by Lando and Doll[20] (structure I), Hasegawa et al.[21] (structure II), and Takahashi et al.[23] (structure III). As expected, the analysis of Bachmann and Lando,[22] which supports structure II in terms of conformation, leads to almost the same jump angles, the maximum deviation being 0.5°. Note that motions 2 and 5 give two distinct jump angles because, in these cases, the two ^2H nuclei bonded to the same carbon reorient by different angles. The chain packing of structure I leading to a non-zero dipole component along the b axis has been shown to be inapplicable.[22,23] However,

we include the conformation of structure I here for comparison since it corresponds to an exact TGTḠ sequence.[20] Such a chain conformation gives, as expected, some jump angles that are very close to either the tetrahedral angle or its complement (Table I). Indeed, disregarding possible translations, motions 3, 4, 7, and 8 can then be considered to be possible on a tetrahedral lattice.[31] On the other hand, the distorted TGTḠ conformation of structure II leads to jump angles departing up to 26° from 109.4 and 70.6°. For the slightly distorted TGTḠ conformation III, however, motions 3, 4, 7, and 8 give jump angles that are quite close to 109.4 or 70.6°. Moreover, Table I shows that the exact TGTḠ conformation (I) and, particularly, the distorted TGTḠ conformation (II) cannot provide an agreement with our NMR results. In the case of the latter, the angular discrepancies are as large as 19°, while for the former there is a discrepancy of at least 4°. Both of these are significant considering the high angular resolution offered by 2D exchange ^2H NMR (±0.5°).[16] On the other hand, for structure III, motions 4 and 7 remarkably provide the *exact* angles observed by 2D NMR (67 and 113°) while motions 3 and 8 lead to a difference of only 1° with our NMR results (68 and 112°) (Table I). Since we have detected experimentally a small distribution of ±3° width around the 67° peak in the RAD, and because of possible small deviations in the precise crystalline structure, we cannot reasonably exclude motions 3 and 8 on the basis of a 1° deviation. At this point, it can nevertheless be concluded that our NMR results are clearly in agreement with the crystalline structure given by Takahashi et al.[23] (III) but show discrepancies with structures I[20] and II.[21]

Obviously, we need additional information in order to determine which motion (3, 4, 7, or 8?) actually occurs at the α-relaxation of PVF_2. First, we should note that some of these motions have already been proposed to occur in PVF_2. Indeed, motion 3 can be completed by elementary three-bond motions[31] that are believed to be the mechanism governing the thermally induced transition from the α- to the γ-phase.[32,33] Motion 4 has been proposed by Lovinger[34] to explain the transition from the α- to the δ-phase by the application of an electric field. However, motions 3, 4, 7, and 8 all result in a different dipole-moment transition. Therefore, these motions should be differentiated by dielectric relaxation spectroscopy. Indeed, in an ingenious study of the anisotropy of the dielectric relaxation, Miyamoto et al.[5] were able to demonstrate that the dipole moment changes its orientation only along the *c* axis, thus implying that the α-relaxation is of the type AC ↔ AC̄. Moreover, this finding has been supported by the fine-level X-ray analysis of Takahashi and Miyaji.[7] Table I shows that only two molecular motions, 5 and 7, lead to the AC ↔ AC̄ transition. Since motion 5, which involves the conformational change TGTḠ ↔ GTḠT, can clearly be excluded by our NMR results (Table I), the α-relaxation must be due to motion 7, which is completed by the chain isomerization TGTḠ ↔ ḠTGT (Figure 6) and leads to a jump angle of 113°, in excellent agreement with our NMR results. Although the final state RAD shows that all the chain segments must reorient, it is very unlikely that such a motion occurs in a single step for the whole chain of a crystal because of too high an activation energy. As already proposed,[5,8] it should be accomplished through local conformational rearrangements, leaving at any time the major portion of the chain unchanged, e.g., by diffusion of defects or kinks along the chain. Since the α-relaxation is strongly influenced by the level of heterolinkages,[3] the concentration of conformational defects is expected to be related to the content of tail–tail and head–head junctions, which is minimized in our specimens.

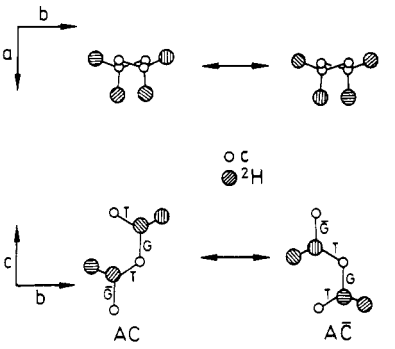

Figure 6. Unique molecular motion consistent with the NMR, X-ray, and dielectric results. Projections in the *ab* plane (top) and *bc* plane (bottom). The ^2H atoms are differentiated to show that each C–^2H bond of the repeat unit is jumping by the same angle of 113°. Fluorine atoms have been omitted for clarity.

Furthermore, it must be pointed out that motions 3, 4, and 8 may also be excluded on other grounds. Motions 4 and 8 that involve dipole-moment reversal along *a* (i.e., to parallel packing) are implausible on thermodynamic grounds, which would tend to favor antiparallel dipoles. Moreover, it is known from poling at room temperature that it takes very high energy to change the antipolar α-phase to its polar counterpart (δ-phase).[35,36] Motion 3 completed through elementary three-bond motions would necessitate the creation of a γ-like intermediate conformation (TḠTGTḠTG ↔ TTTGTTTḠ), at least locally.[33,37] This is also improbable because the α-phase transforms to the γ-phase only at very high temperatures and extremely slowly.[37]

Conclusions

In the crystalline α-phase of PVF_2, 2D exchange ^2H NMR directly detects ultraslow chain motions at 370 K reorienting the C–^2H bond directions by the uniquely defined angles of 67 or 113°. Moreover, the time scale of these motions agrees well with the so-called α-relaxation detected by dielectric and mechanical spectroscopy. Considering the published X-ray data, these NMR results are consistent only with the conformation of Takahashi et al.[23] Four different models of molecular motion are in agreement with the jump angles determined by NMR, and these have been considered in detail here. However, these molecular motions could be differentiated in terms of their electrical properties. Of the four possible motions, only one is in agreement with the dielectric relaxation results of Miyamoto et al.[5] It is defined by the dipole moment transition AC ↔ AC̄ and the conformational change TGTḠ ↔ ḠTGT, yielding an effective dipole-moment reversal only along the chain axis and a reorientation angle of 113° for the C–^2H bond directions.

Acknowledgment. We are very grateful to Mrs. J. Kometani of AT&T Bell Laboratories for provision of the deuterated specimen. We also thank Professor J. B. Lando for his comments on the manuscript. J. Hirschinger thanks the Max-Planck-Gesellschaft for a stipend. Financial support of the Deutsche Forschungsgemeinschaft (SFB 262) is gratefully acknowledged.

References and Notes

(1) Lovinger, A. J. In *Developments in Crystalline Polymers*; Bassett, D. C., Ed.; Applied Science Publishers: London, 1981; Vol. 1, p 195.

(2) Broadhurst, M. G.; Davis, G. T.; McKinney, J. E.; Collins, R. E. *J. Appl. Phys.* **1978**, *49*, 4992.
(3) Yano, S. *J. Polym. Sci.: Polym. Phys. Ed.* **1970**, *8*, 1057.
(4) Nakagawa, K.; Ishida, Y. *J. Polym. Sci.: Polym. Phys. Ed.* **1973**, *11*, 1503.
(5) Miyamoto, Y.; Miyaji, H.; Asai, K. *J. Polym. Sci.: Polym. Phys. Ed.* **1980**, *18*, 597.
(6) McBrierty, V. J.; Douglass, D. C.; Weber, T. A. *J. Polym. Sci.: Polym. Phys. Ed.* **1976**, *14*, 1271.
(7) Takahashi, Y.; Miyaji, K. *Macromolecules* **1983**, *16*, 1789.
(8) Clark, J. D.; Taylor, P. L.; Hopfinger, A. J. *J. Appl. Phys.* **1981**, *52*, 5903.
(9) Spiess, H. W. In *Developments in Oriented Polymers*; Bassett, D. C., Ed.; Applied Science Publishers: London, 1982; Vol. 1, p 72. Spiess, H. W. In *Advances in Polymer Science*; Kausch, H. H., Zachmann, H. G., Eds.; Springer: Berlin, 1985; Vol. 66, p 23.
(10) Blümich, B.; Spiess, H. W. *Angew. Chem., Int. Ed. Engl.* **1988**, *27*, 1655.
(11) Schmidt, C.; Blümich, B.; Spiess, H. W. *J. Magn. Reson.* **1988**, *79*, 269.
(12) Wefing, S.; Spiess, H. W. *J. Chem. Phys.* **1988**, *89*, 1219.
(13) Wefing, S.; Kaufmann, S.; Spiess, H. W. *J. Chem. Phys.* **1988**, *89*, 1234.
(14) Kaufmann, S.; Wefing, S.; Schaefer, D.; Spiess, H. W. *J. Chem. Phys.* **1990**, *93*, 197.
(15) Hagemeyer, A.; Schmidt-Rohr, K.; Spiess, H. W. *Adv. Magn. Reson.* **1989**, *13*, 85.
(16) Hagemeyer, A.; Brombacher, L.; Schmidt-Rohr, K.; Spiess, H. W. *Chem. Phys. Lett.* **1990**, *167*, 583.
(17) Schaefer, D.; Spiess, H. W.; Suter, U. W.; Fleming, W. W. *Macromolecules* **1990**, *23*, 3421.
(18) Mehring, M. *Principles of High Resolution NMR in Solids*, 2nd ed.; Springer: Berlin, 1983.
(19) Doverspike, M. A.; Conradi, M. S.; DeReggi, A. S.; Cais, R. E. *J. Appl. Phys.* **1989**, *65*, 541.
(20) Doll, W. W.; Lando, J. B. *J. Macromol. Sci.-Phys.* **1970**, *B4*, 309.
(21) Hasegawa, R.; Takahashi, Y.; Chatani, Y.; Tadokoro, H. *Polym. J.* **1972**, *3*, 600.
(22) Bachmann, M. A.; Lando, J. B. *Macromolecules* **1981**, *14*, 40.
(23) Takahashi, Y.; Matsubara, Y.; Tadokoro, H. *Macromolecules* **1983**, *16*, 1588.
(24) Spiess, H. W. *NMR—Basic Principles and Progress*; Springer: Berlin 1978; Vol. 15, p 55.
(25) Ernst, R. R.; Bodenhausen, G.; Wokaun, A. *Principles of NMR in One and Two Dimensions*; Clarendon: Oxford, 1987.
(26) Cais, R. E.; Kometani, J. M. *Macromolecules* **1984**, *17*, 1887.
(27) Takase, Y.; Tanaka, H.; Wang, T. T.; Cais, R. E.; Kometani, J. M. *Macromolecules* **1987**, *20*, 2320.
(28) Lausch, M.; Spiess, H. W. *J. Magn. Reson.* **1983**, *54*, 466.
(29) English, A. D. *Macromolecules* **1984**, *17*, 2182.
(30) Hirschinger, J.; Miura, H.; Gardner, K. H.; English, A. D. *Macromolecules* **1990**, *23*, 2153.
(31) Monnerie, L.; Geny, F. *J. Chim. Phys.* **1969**, *66*, 1691.
(32) Lovinger, A. J. *J. Appl. Phys.* **1981**, *52*, 5934.
(33) Takahashi, Y.; Matsubara, Y.; Tadokoro, H. *Macromolecules* **1982**, *15*, 334.
(34) Lovinger, A. J. *Macromolecules* **1981**, *14*, 225.
(35) Davis, G. T.; McKinney, J. E.; Broadhurst, M. G.; Roth, S. C. *J. Appl. Phys.* **1978**, *49*, 4998.
(36) Lovinger, A. J. *Macromolecules* **1982**, *15*, 40.
(37) Lovinger, A. J. *Polymer* **1980**, *21*, 1317.

Registry No. PVF_2, 24937-79-9.